CHIN. PHYS. LETT. Vol. 37, No. 4 (2020) 044204

Optical Properties of Atomic Defects in Hexagonal Boron Nitride Flakes under High Pressure *

Xiao-Yu Zhao(赵晓宇)[1,2], Jun-Hui Huang(黄君辉)[1,2], Zhi-Yao Zhuo(卓志瑶)[1,2], Yong-Zhou Xue(薛永洲)[1], Kun Ding(丁琨)[1], Xiu-Ming Dou(窦秀明)[1,2**], Jian Liu(刘剑)[1,2], Bao-Quan Sun(孙宝权)[1,2]

[1]*State Key Laboratory for Superlattices and Microstructures, Institute of Semiconductors, Chinese Academy of Sciences, Beijing 100083*

[2]*College of Materials Science and Optoelectronic Technology, University of Chinese Academy of Sciences, Beijing 100049*

(Received 27 November 2019)

We investigate the pressure spectral characteristics and the effective tuning of defect emissions in hexagonal boron nitride (hBN) at low temperatures using a diamond anvil cell (DAC). It is found that the redshift rate of emission energy is up to 10 meV/GPa, demonstrating a controllable tuning of single photon emitters through pressure. Based on the distribution character of pressure coefficients as a function of wavelength, different kinds of atomic defect states should be responsible for the observed defect emissions.

PACS: 42.50.Dv, 61.72.−y, 62.50.−p, 78.67.−n DOI: 10.1088/0256-307X/37/4/044204

Recently, due to the discoveries of ultrabright and stable single-photon emitters (SPEs) under ambient conditions in hexagonal boron nitride (hBN), atomic defects in hBN have sparked immense interest in one of the most promising quantum light sources for quantum cryptography as well as spin-based quantum bits, which is similar to recent advances in nitrogen-vacancy centers in diamond.[1−8] Moreover, owing to a wide bandgap two-dimensional (2D) material, atomic-scale thickness enables the SPEs in hBN to have huge potential application for strongly coupling to plasmonic and metallic dielectric antennas,[9−11] which makes them especially useful for hybrid quantum devices. However, the origin of broad spectral range of SPEs in hBN remains a subject of debate in spite of many efforts having been carried out to promote the efficient control, such as the deterministic formation of defects via controlled edge creation,[12] CVD growth technique,[13] inducing curvature with nanopillars,[14] and the efficient tuning through strain or Stark effect.[15−18] Up to date, many theoretical calculations have shown that different types of atomic defects such as N- or B-vacancies or substitutions with carbon or oxygen may exist.[19,20] Experimentally, it has been shown that the local stain distributions or trapped charges near the color center may induce the spectral shift.[14,15,17,18] Thus different types of atomic defects combined with local strain or trapped charges should be responsible for the broad spectral emissions.[21] Here, to explore the various types of defect emissions and local environments of atomic defects in hBN, hydrostatic pressure technique is employed to tune inter-layer coupling and local strain or trapped charged states.[22]

In this Letter, the pressure responses of defect emissions in hBN are investigated under hydrostatic pressure. It is found that a distribution of pressure coefficients of 26 emitters is from −1 to −12 meV/GPa. The corresponding wavelengths of defect emissions cover the range from about 570 to 710 nm, which are approximately distributed in three central wavelength regions. In addition, the spectral stability of emission lines and emission intensities are measured under pressure.

We prepared hBN samples from an ethanol/water solution with nanosized pristine flakes purchased from Graphene Supermarket. Their lateral size distribution ranges from 50 to 200 nm, and the thickness ranges from 1 to 5 monolayers. Photoluminescence (PL) measurements under high pressure at 20 K were performed using an improved diamond anvil cell (DAC).[23,24] A condensed argon was used as a pressure-transmitting medium at low temperature. For the experiments, the first step was to prepare a bare SiO_2/Si substrate mechanically thinned to a total thickness of approximately 20 μm. Then we dropped a small amount of hBN flake solution on the SiO_2/Si wafer, let it dry in air and finally we cut the SiO_2/Si wafer containing hBN multilayer flakes into pieces of approximately $100 \times 100\ \mu m^2$ in size to fit the DAC chamber. Micro-PL measurements were taken at low temperature using a home-built optical confocal microscopy setup, and a 532 nm laser with a power of a few mW was focused on the sample in the DAC device using an objective (NA = 0.35). The emitted PL was collected by the same objective and analyzed using a 0.5 m monochromator equipped with a silicon charge-coupled device (CCD). Additionally, a Hanbury Brown and Twiss (HBT) setup equipped with two silicon avalanche photodiodes (APDs) was used to perform autocorrelation measurements for calibrating single photon emission characteristics.

*Supported by the Postdoctoral Science Foundation of China under Grant No. Y8T0111001.

**Corresponding author. Email: xmdou04@semi.ac.cn

© 2020 Chinese Physical Society and IOP Publishing Ltd

Figure 1(a) shows an optical microscope image of hBN flakes deposited on a Si/SiO_2 substrate, and the inset is a picture of pristine hBN flakes in solution. Note that a large spectral distribution of PL has been reported by many works.[2,3,12–18] As shown in Fig. 1(b), it is a typical PL spectrum with a central wavelength of 658.17 nm and corresponding single-photon character, second-order autocorrelation function $g^2(\tau)$, is measured through an HBT setup. Its $g^2(\tau)$ data are fitted using an equation of $g^2(\tau) = 1 - a \times e^{|\tau|/t}$, where parameter a is the fitting parameter, and t is the fitting lifetime of the excited state of defects. The fitting $g^2(\tau)$ value at zero delay time is 0.05 and the lifetime is 0.8 ns, confirming that the defect acts as a single-photon emitter.

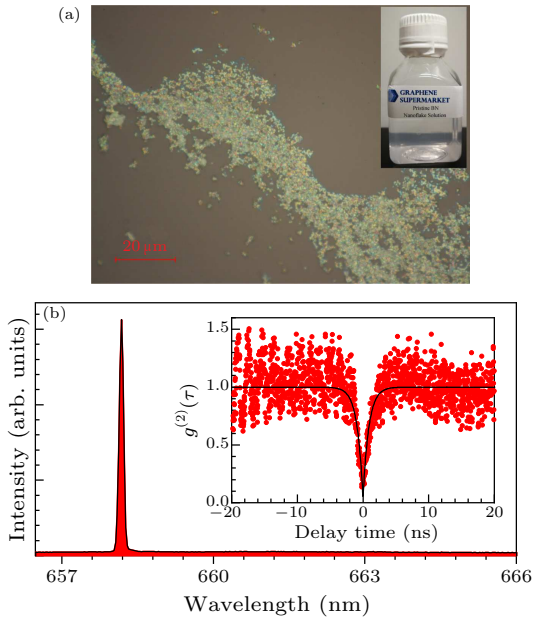

Fig. 1. (a) Optical microscope image of hBN flakes. Inset: A picture of pristine hBN flakes in solution. (b) PL spectrum of defect emission line at a wavelength of 658 nm. Inset: Second-order correlation functions $g^2(\tau)$ with a $g^2(0)$ value of 0.05.

Figure 2(a) presents the distribution of pressure coefficients from 26 different emitters with different emission wavelengths distributed in the range 570–710 nm. The corresponding pressure coefficients are approximately ranged from −1 to −12 meV/GPa. It is worthy to note that 18 of the 26 defect lines are approximately distributed in the I, Ⅱ and Ⅲ regions, corresponding to the wavelength of 580 ± 5, 610 ± 5 and 650 ± 5 nm, respectively, marked by green broadband. The possible defect states responsible for the emission lines are due to the anti-site nitrogen vacancy complex defects in multilayer hBN.[16] Within each region, it includes different pressure coefficients, which should correspond to the defects from 2 to 5 monolayers or/and Stark shifting stemming from a trapped charge near a defect center as well as a local strain distribution in the crystal.[21] In our previous work, it is found that a larger difference in the pressure coefficient has originated from defect states in different layers,[16] i.e., as the number of layers increases, the absolute value of the pressure coefficient becomes larger. The fluctuation of the smaller pressure coefficient in Fig. 2(a) should come from the defects due to complex local environments, such as local strain or a trapped charged states. In Fig. 2(b), it is a typical pressure-induced emission energy redshift at a rate of 10 meV/GPa for applied pressure from 0.6 and 2.5 GPa. It shows an effective tuning method of single-photon emitters of defects in hBN through pressure. The solid circles can be fitted by a linear function of $y = Ax + B$, resulting in a pressure coefficient of −10 meV/GPa. The corresponding PL at 0.69 GPa is shown in the inset of Fig. 2(b).

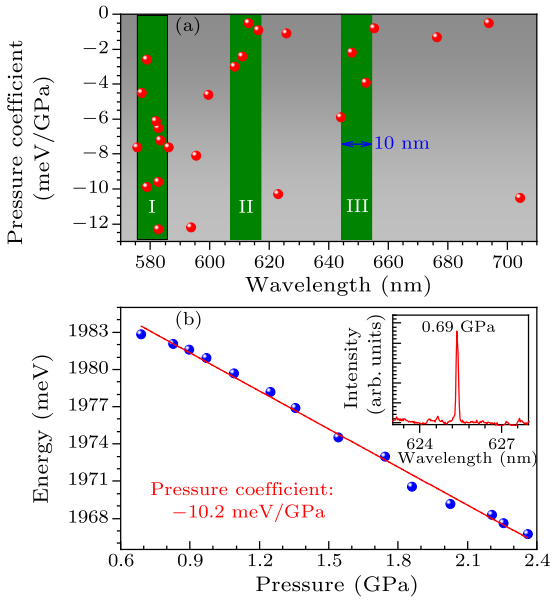

Fig. 2. (a) Distribution of pressure coefficients from 26 different emitters as a function wavelength ranging roughly from 570 to 710 nm. The width of green color area of I, Ⅱ and Ⅲ regions is 10 nm. (b) PL peak energy as a function of pressure from 0.6 to 2.5 GPa. The blue solid circles present a redshift of the emission energies, which are fitted by linear functions, yielding a pressure coefficient of 10.2 meV/GPa. Inset: PL spectrum at 0.69 GPa.

Next, the fluorescence stability of atomic defects in hBN under high pressure has been studied. Figure 3(a) presents the pressure-dependent PL lines of defects as the pressure increases from 0.60 to 2.87 GPa. It is shown that the PL spectral line in the vicinity of 613 nm has a slight redshift and the PL spectral line cannot be observed in the vicinity of 620 nm when the pressure is up to 0.83 GPa. A time evolution of the PL peak wavelength and intensity are measured at 0.60 and 2.87 GPa for lasting 500 s, respectively, as shown in Fig. 3(b). Here the excitation power is about 1.3 mW, each PL spectral integration time is 1 s and the wavelength interval of the ordinate is 10 nm. It clearly demonstrates a remarkable PL intensity fluctuation observed in the vicinity of 620 nm at a pressure of 0.60 GPa; i.e., the so-called spectral diffusion.

This is possible due to the trapped carrier induced Stark shifts,[17] owing to the increasing probability of trapping carriers near defect states as the pressure increases. It is found that a fluctuation range of emission wavelength is about 3 nm, meaning that the possible wavelength shift induced by the trapped carriers near the emission defects should be small. This explanation is consistent with the observed small shifts of pressure coefficient and emission wavelength as presented in Fig. 2(a). In contrast, however, the PL line observed in the vicinity of 613 nm is very stable and has an obvious redshift at higher pressure. However, its PL intensity becomes to decrease as the pressure is up to 2.87 GPa. It can be seen in Fig. 3(a) that actually the PL intensity increases in the first stage as pressure increases from 0.60 to 1.38 GPa, and then its intensity turns to decrease with further increase of pressure. Recently, it was reported that the excitation wavelength dependences of defect emissions have proved that the defect emitters have a very complex level scheme, which cannot be described by a simple two- or three-level system.[25,26] Thus, according to this understanding, the observed PL intensity variations of atomic defects under pressure should be concerned with the complex variations of defect level states, nearby trapped carrier states and interlayer couplings.

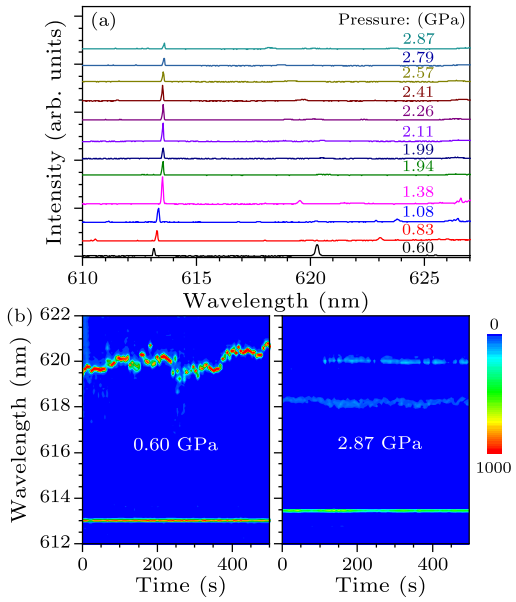

Fig. 3. (a) Defect emission lines measured under pressures from 0.60 to 2.87 GPa. PL line of 613 nm showing a slight redshift and PL line of 620 nm quenching with the increasing pressure up to 0.83 GPa. (b) Time-dependent PL spectra at 0.60 and 2.87 GPa, respectively, showing a seriously spectral fluctuation at a wavelength of ∼620 nm.

Further experimental results of pressure-induced PL peak wavelength shifts and intensity variations are presented in Fig. 4 under pressure from 0.60 to 2.87 GPa. It shows that PL emission peaks become stronger when the applied pressure is up to 2.87 GPa and the emission lines on the left (right) exhibit a redshift (blue shift), respectively. Here, as reported in our previous article, a blue shift of the PL line as a function of pressure is related to the defect emissions in monolayer, while the redshift one corresponds to the defects of multilayers. In addition, the time-dependent PL spectral measurements at 0.60 and 2.87 GPa, as shown in Fig. 4(b), show that the PL spectra is stable and the PL intensities become stronger at higher pressure.

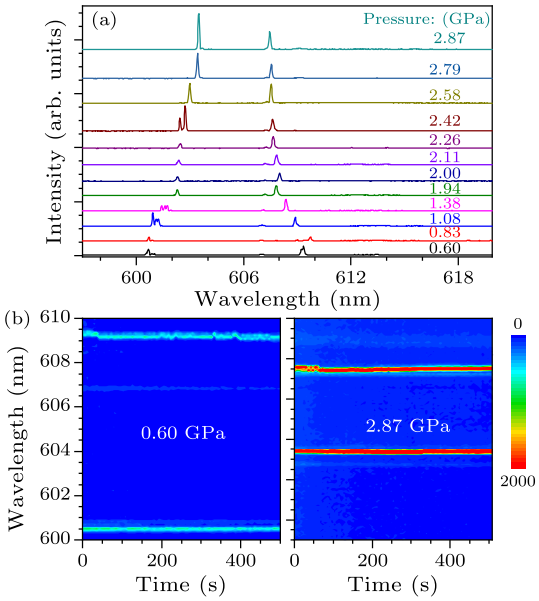

Fig. 4. (a) Defect emission lines measured under pressures from 0.60 to 2.87 GPa, showing a redshift (blue shift) of emission lines on the left (right), respectively. (b) Time-dependent PL spectra at 0.60 and 2.87 GPa, respectively, showing that the PL spectra is stable.

In summary, we have studied the atomic defect emissions in multilayer hBN flakes using an electrically driven DAC at low temperature. The experimental results show that the single defect emission corresponds to a single photon source with a $g^2(0)$ value of 0.05, and its emission wavelength can be tuned at a rate of 10 meV/GPa. Based on the distributions of emission wavelengths and pressure coefficients, we speculate that different kinds of atomic defect states should be responsible for the observed defect emissions. Indeed, theoretical calculations are needed to further confirm the observed results and to designate the types of atomic defects.

References

[1] Tran T T, Bray K, Ford M J, Toth M and Aharonovich I 2016 *Nat. Nanotechnol.* **11** 37
[2] Tran T T, Elbadawi C, Totonjian D, Lobo C J, Grosso G, Moon H, Englund D R, Ford M J, Aharonovich I and Toth M 2016 *ACS Nano* **10** 7331
[3] Jungwirth N R, Calderon B, Ji Y, Spencer M G, Flatté M E and Fuchs G D 2016 *Nano Lett.* **16** 6052
[4] Bourrellier R, Meuret S, Tararan A, Stéphan O, Kociak M, Tizei L H G and Zobelli A 2016 *Nano Lett.* **16** 4317
[5] Kianinia M, Regan B, Tawfik S A, Tran T T, Ford M J, Aharonovich I and Toth M 2017 *ACS Photon.* **4** 768

[6] Konthasinghe K, Chakraborty C, Mathur N, Qiu L, Mukherjee A, Fuchs G D and Vamivakas A N 2019 *Optica* **6** 542
[7] Gottscholl A, Kianinia M, Soltamov V, Bradac C, Kasper C, Krambrock K, Sperlich A, Toth M, Aharonovich I and Dyakonov V 2019 arXiv:1906.03774v1[physics.optics]
[8] Jelezko F and Wrachtrup J 2006 *Phys. Status Solidi* **203** 3207
[9] Tran T T, Wang D, Xu Z Q, Yang A, Toth M, Odom T W and Aharonovich I 2017 *Nano Lett.* **17** 2634
[10] Nguyen M, Kim S, Tran T T, Xu Z Q, Kianinia M, Toth M and Aharonovich I 2018 *Nanoscale* **10** 2267
[11] Li X, Scully R A, Shayan K, Luo Y and Strauf S 2019 *ACS Nano* **13** 6992
[12] Ziegler J, Klaiss R, Blaikie A, Miller D, Horowitz V R and Alemán B J 2019 *Nano Lett.* **19** 2121
[13] Abidi I H, Mendelson N, Tran T T, Tyagi A, Zhuang M, Weng L T, Özyilmaz B, Aharonovich I, Toth M and Luo Z 2019 *Adv. Opt. Mater.* **7** 1900397
[14] Proscia N V, Shotan Z, Jayakumar H, Reddy P, Cohen C, Dollar M, Alkauskas A, Doherty M, Meriles C A and Menon V M 2018 *Optica* **5** 1128
[15] Grosso G, Moon H, Lienhard B, Ali S, Efetov D K, Furchi M M, Jarillo-Herrero P, Frod M J, Aharonovich I and Englund D 2017 *Nat. Commun.* **8** 705
[16] Xue Y, Wang H, Tan Q, Zhang J, Yu T, Ding K, Jiang D, Dou X, Shi J and Sun B 2018 *ACS Nano* **12** 7127
[17] Shotan Z, Jayakumar H, Considine C R, Mackoit M, Fedder H, Wrachtrup J, Alkauskas A, Doherty M W, Menon V M and Meriles C A 2016 *ACS Photon.* **3** 2490
[18] Noh G, Choi D, Kim J H, Im D G, Kim Y H, Seo H and Lee J 2018 *Nano Lett.* **18** 4710
[19] Tawfik S A, Ali S, Fronzi M, Kianinia M, Tran T T, Stampfl C, Aharonovich I, Toth M and Ford M J 2017 *Nanoscale* **9** 13575
[20] Korona T and Chojecki M 2019 *Int. J. Quantum Chem.* **119** e25925
[21] Wigger D, Schmidt R, Del Pozo-Zamudio O, Preuß J A, Tonndorf P, Schneider R, Steeger P, Kern J, Khodaei Y, Sperling J, Michaelis de Vasconcellos S, Bratschitsch R and Kuhn T 2019 *2D Mater.* **6** 035006
[22] Gauthier M, Polian A, Besson J M and Chevy A 1989 *Phys. Rev. B* **40** 3837
[23] Wu X, Dou X, Ding K, Zhou P, Ni H, Niu Z, Jiang D and Sun B 2013 *Appl. Phys. Lett.* **103** 252108
[24] Ye Y, Dou X, Ding K, Chen Y, Jiang D, Yang F and Sun B 2017 *Phys. Rev. B* **95** 245313
[25] Jungwirth N R and Fuchs G D 2017 *Phys. Rev. Lett.* **119** 057401
[26] Schell A W, Svedendahl M and Quidant R 2018 *Adv. Mater.* **30** 1704237